AIP | Journal of Applied Physics

Ferroelectricity in yttrium-doped hafnium oxide

J. Müller, U. Schröder, T. S. Böscke, I. Müller, U. Böttger et al.

Citation: J. Appl. Phys. **110**, 114113 (2011); doi: 10.1063/1.3667205
View online: http://dx.doi.org/10.1063/1.3667205
View Table of Contents: http://jap.aip.org/resource/1/JAPIAU/v110/i11
Published by the American Institute of Physics.

Related Articles

Structural incommensurate modulation rule in hexagonal $Ba(Ti_{1-x}M_x)O_{3-\delta}$ (M = Mn, Fe) multiferroics
AIP Advances 2, 042129 (2012)

Water assisted gate induced temporal surface charge distribution probed by electrostatic force microscopy
J. Appl. Phys. 112, 084329 (2012)

Influence of target composition and deposition temperature on the domain structure of $BiFeO_3$ thin films
AIP Advances 2, 042104 (2012)

Nanodomain structures formation during polarization reversal in uniform electric field in strontium barium niobate single crystals
J. Appl. Phys. 112, 064117 (2012)

The effect of the top electrode interface on the hysteretic behavior of epitaxial ferroelectric $Pb(Zr,Ti)O_3$ thin films with bottom $SrRuO_3$ electrode
J. Appl. Phys. 112, 064116 (2012)

Additional information on J. Appl. Phys.

Journal Homepage: http://jap.aip.org/
Journal Information: http://jap.aip.org/about/about_the_journal
Top downloads: http://jap.aip.org/features/most_downloaded
Information for Authors: http://jap.aip.org/authors

ADVERTISEMENT

GoodFellow
metals • ceramics • polymers • composites
70,000 products
450 different materials
small quantities fast
www.goodfellowusa.com

Downloaded 06 Nov 2012 to 131.188.201.33. Redistribution subject to AIP license or copyright; see http://jap.aip.org/about/rights_and_permissions

Ferroelectricity in yttrium-doped hafnium oxide

J. Müller,[1,a)] U. Schröder,[2,b)] T. S. Böscke,[3,b)] I. Müller,[4] U. Böttger,[4] L. Wilde,[1]
J. Sundqvist,[1,b)] M. Lemberger,[5] P. Kücher,[1] T. Mikolajick,[2,6] and L. Frey[5,7]
[1]*Fraunhofer Center Nanoelectronic Technologies (CNT), 01099 Dresden, Germany*
[2]*Namlab gGmbH, 01187 Dresden, Germany*
[3]*Löberwallgraben 2, 99096 Erfurt, Germany*
[4]*RWTH Aachen, Institut für Werkstoffe der Elektrotechnik, 52074 Aachen, Germany*
[5]*Fraunhofer Institute for Integrated Systems and Device Technology (IISB), 91058 Erlangen, Germany*
[6]*Chair of Nanoelectronic Materials, University of Technology Dresden, 01062 Dresden, Germany*
[7]*Chair of Electron Devices, University of Erlangen-Nürnberg, 91058 Erlangen, Germany*

(Received 23 September 2011; accepted 5 November 2011; published online 7 December 2011)

Structural and electrical evidence for a ferroelectric phase in yttrium doped hafnium oxide thin films is presented. A doping series ranging from 2.3 to 12.3 mol% $YO_{1.5}$ in HfO_2 was deposited by a thermal atomic layer deposition process. Grazing incidence X-ray diffraction of the 10 nm thick films revealed an orthorhombic phase close to the stability region of the cubic phase. The potential ferroelectricity of this orthorhombic phase was confirmed by polarization hysteresis measurements on titanium nitride based metal-insulator-metal capacitors. For 5.2 mol% $YO_{1.5}$ admixture the remanent polarization peaked at 24 $\mu C/cm^2$ with a coercive field of about 1.2 MV/cm. Considering the availability of conformal deposition processes and CMOS-compatibility, ferroelectric Y:HfO_2 implies high scaling potential for future, ferroelectric memories. © *2011 American Institute of Physics*. [doi:10.1063/1.3667205]

INTRODUCTION

Ferroelectric memories are an extremely interesting approach to nonvolatile data storage, since they show a unique combination of very fast, low power writing with nonvolatile retention that is unmatched by charge based and other emerging concepts like magnetoresistive RAM's, phase change memories and resistive RAM's. Up till now mainly lead zirconate titanate (PZT) was used for the fabrication of ferroelectric memories.[1] However, PZT is quite complicated to integrate into a CMOS process and therefore the scaling has been much slower than the scaling of conventional charge based memories. This results in much higher production cost for ferroelectric memories compared to competing charge based technologies.

Integrating thin layers of doped HfO_2 on the other hand, has already become well-known to microelectronic engineering, since stabilization of the higher-k cubic (*Fm3 m*) or tetragonal ($P4_2/nmc$) phase in the otherwise monoclinic ($P2_1/c$) HfO_2[2] is of considerable interest to dielectric scaling in the manufacturing of CMOS[3] and DRAM[4] devices. Recently, it has been demonstrated that doping of HfO_2 thin films with SiO_2[5] or ZrO_2[6] does not only stabilizes the tetragonal phase, but can also produce a spontaneous polarization at intermediate doping levels, that results in usable, ferroelectric hysteresis loops in these layers.

Phase stability in HfO_2, however, can also be influenced by $YO_{1.5}$ admixture. As predicted by first principles calculations on trivalent dopants, stabilization of cubic HfO_2 can be achieved for moderate yttrium doping.[7] Analogous to the well-known yttrium stabilized zirconia (YSZ),[8] successful stabilization of the cubic phase in epitaxial, as well as polycrystalline Y:HfO_2 thin films has been presented by several authors.[9–17] Reported doping levels for complete stabilization of the cubic phase in HfO_2 range from 4 to 17 mol% $YO_{1.5}$ admixture, thereby achieving k-values of about 18 to 32.

However, the exact nature of the crystalline phases that form close to the stability region of the cubic phase remains unclear. The bulk phase diagram allows for a monoclinic to cubic phase transition by passing through a coexistence region of both phases.[18] At temperatures above 1350 K, an intermediate tetragonal phase has to be considered. However, when Y:HfO_2 is crystallized by rapid thermal processes (RTP) with fast cooling rates, such as those utilized in microelectronic applications, the diffusion of dopant atoms is limited and a number of metastable phases can be formed. Yashima *et al*.[19] and Fujimori *et al*.[20] observed metastable tetragonal phases (t' and t'') in quenched Y:HfO_2 bulk samples between 10 and 13 mol% $YO_{1.5}$. Furthermore, they described the occurrence of two lower symmetry phases, γ_1 and γ_2, that were only identifiable by Raman Spectroscopy for lower $YO_{1.5}$ admixture. In addition, recent publications report the existence of a possibly orthorhombic/monoclinic phase mixture that forms prior to complete stabilization of the cubic phase in Y:HfO_2 thin films.[21,22]

In this paper we investigate the electronic properties of metastable crystalline phases in Y:HfO_2 thin films, and report the observation of ferroelectricity. We demonstrate that a spontaneous polarization in HfO_2 can be provoked by $YO_{1.5}$ admixture, while at the same time easing some of the processing constrains present in the previously published systems. On the basis of a structural investigation we claim that this crystal property originates from a non-centrosymmetric orthorhombic phase located close to the stability region of

a)Author to whom correspondence should be addressed. Electronic mail: johannes.mueller@ieee.org.
b)T. S. Böscke, U. Schröder, and J. Sundqvist were with Qimonda Dresden, Dresden, Germany while the initial experimental work was performed.

 © 2011 American Institute of Physics

Downloaded 06 Nov 2012 to 131.188.201.33. Redistribution subject to AIP license or copyright; see http://jap.aip.org/about/rights_and_permissions

the cubic phase. Y:HfO_2 thin films have a large bandgap,[11] are temperature stable,[21] CMOS compatible,[23,24] and due to the availability of mature atomic layer deposition (ALD) processes,[13] they are capable of conformal 3D integration. Therefore Y:HfO_2 is considered a promising material for future, highly scaled ferroelectric memories.

EXPERIMENTAL

Y:HfO_2 thin films were deposited by thermal ALD on 300 mm Si substrates that, prior to dielectric deposition, received a 18 nm chemical vapor deposited (CVD) TiN ($TiCl_4/NH_3$) bottom electrode in a batch furnace. The ALD process was based on the commercially available metal organic precursors tetrakis(ethylmethylamino)hafnium (TEMAH) and tris(methylcyclopentadienyl)yttrium ($Y(MeCp)_3$). Ozone was used as the oxidant and argon as the purge and carrier gas. The $YO_{1.5}$ content in HfO_2 was defined by varying the cycle ratio of the precursors and monitored by inline X-ray photoelectron spectroscopy (XPS) and Rutherford backscattering (RBS). A constant thickness of 10 nm for all films was achieved by adjusting the number of Hf:Y super cycles, and was confirmed by inline spectral ellipsometry and HR-TEM. Crystallization of the as deposited amorphous Y:HfO_2 thin films was induced by a $600\,^{\circ}C/20\,s/N_2$ RTP step, referred to in text as post deposition anneal (PDA). Samples annealed after room temperature deposition of a 4 nm physical vapor deposited (PVD) TiN top electrode are referred to in the text as samples treated with post metallization anneal (PMA). Samples with yttrium concentrations ranging from 2.3 to 12.3 mol% $YO_{1.5}$ in HfO_2 were manufactured using both schemes (Fig. 1(a)). This allowed access to the range of metastable phases formed from almost pure hafnium oxide to fully cubic Y:HfO_2. Grazing incidence X-ray diffraction (GI-XRD) on crystalline and high temperature X-ray diffraction (HT-XRD) on as deposited Y:HfO_2 thin films was measured on a Bruker D8 Discover diffractometer using Cu K-alpha radiation from a Cu tube operated at 40 kV/40 mA. The incident angle was set to 0.5°. For HT-XRD analysis, samples were heated from room temperature to 650 °C under constant nitrogen purging in a furnace covered with a hemispherical beryllium dome. During temperature ramp up, *in situ* GI-XRD measurements were performed.

For electrical measurements, Pt dots were evaporated on to the TiN top electrode, forming structured metal-insulator-metal (MIM) capacitors in a subsequent etching step. For samples that received PDA treatment, Pt dots were directly evaporated on top of the Y:HfO_2 thin film. Polarization hysteresis was characterized using an aixACCT TF Analyzer 2000 system and a custom built setup at a frequency of 1 kHz. The small signal capacitance-voltage characteristics of the MIM capacitors were determined with an Agilent 4284 LCR Meter. Typical measurement conditions were a frequency of 10 kHz and a 50 mV ac probing signal on device areas of $1.15*10^{-4}\,cm^2$.

RESULTS AND DISCUSSION

The controlled incorporation of $YO_{1.5}$ into HfO_2 can be realized by the variation of the TEMAH to $Y(MeCp)_3$[12,13,17] precursor pulsing ratio during the ALD process. RBS measurements on as deposited films reveal a linear correlation between precursor cycling ratio and $YO_{1.5}$ incorporation (Fig. 2). Figure 1(b) shows a HR-TEM micrograph of the complete MIM stack after thermal treatment. The polycrystalline structure of the Y:HfO_2, as well as the TiN metal electrode, is clearly visible. Additional HT-XRD experiments confirmed no significant influence of $YO_{1.5}$ content on the crystallization temperature (Fig. 3), which is in good

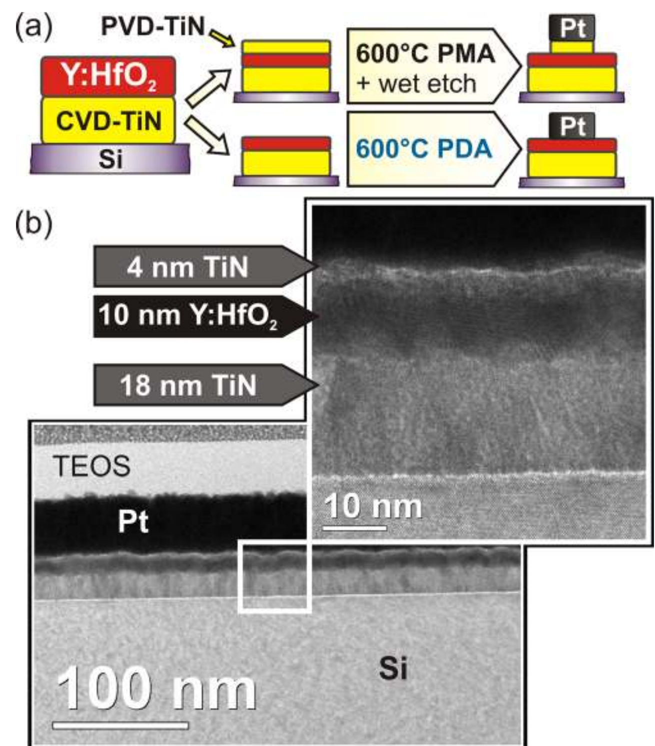

FIG. 1. (Color online) (a) Fabrication flow of MIM capacitors based on atomic layer deposited Y:HfO_2 dielectrics with post deposition anneal (PDA) or post metallization anneal (PMA) in N_2 atmosphere. (b) TEM micrograph and HRTEM enlargement of the fully crystalline TiN/Y:HfO_2/TiN MIM stack on silicon treated with PMA.

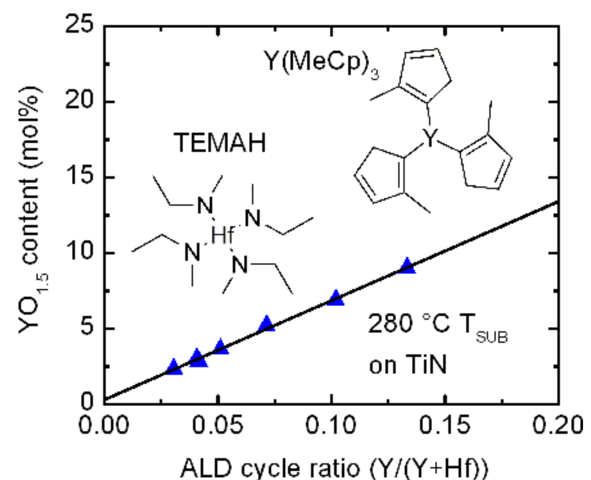

FIG. 2. (Color online) RBS measurements on 10 nm thick films reveal a linear incorporation of $YO_{1.5}$ into HfO_2 with ALD cycle ratio of TEMAH and $Y(MeCp)_3$ precursor. Structural drawings of the metal organic precursors are given.

Downloaded 06 Nov 2012 to 131.188.201.33. Redistribution subject to AIP license or copyright; see http://jap.aip.org/about/rights_and_permissions

agreement with literature data.[9] The crystallization temperature was approximately 400 °C for all of the $YO_{1.5}$ concentrations investigated. Based on these data, complete crystallization of the as deposited amorphous dielectric was induced by a RTP step at 600 °C in samples that were prepared for electrical characterization. This is a significant improvement to the $Hf_{1-x}Zr_xO_2$ system that, depending on the ZrO_2 content, suffers from premature crystallization during deposition, resulting in considerable interface roughening.[25] Due to the higher crystallization temperature of Y:HfO_2, crystallization can either be induced before (PDA) or after (PMA) top electrode deposition (Fig. 1(a)).

Polarization-voltage hysteresis measurements of a 10 nm HfO_2 sample with 5.2 mol% $YO_{1.5}$ admixture are shown in Fig. 4(a). A remanent polarization P_r of 24 μC*cm^{-2} and a coercive field of 1.2 MV*cm^{-1} were observed. Unsaturated polarization hysteresis loops occur when excitation voltages below 4 V are used. This so called sub loop behavior is typical for ferroelectric materials and, as in this case, is usually accompanied by a drop in remanent polarization and coercive field with decreasing excitation signal.[26]

Further proof for the ferroelectric nature of Y:HfO_2 thin films is given by their non-linear small signal capacitance-voltage response. Two capacitance maxima in the vicinity of the coercive field values are observed when a full hysteresis loop is swept (Fig. 4(b)). These maxima are a well-known property of ferroelectric capacitors and are attributed to an increased domain wall movement at the coercive fields.[27]

As can be seen from the polarization hysteresis measurements in Fig. 5 and the summarized polarization values in Fig. 6(a), a gradual transition from a linear dielectric to a ferroelectric response can be observed with decreasing $YO_{1.5}$ content in HfO_2. When the $YO_{1.5}$ content is lowered further, the polarization starts to decline and the coercive field increases. A similar trend is observed for the dielectric constant (Fig. 6(b)). Due to the stabilization of the higher-k cubic phase instead of the lower-k monoclinic phase with increasing $YO_{1.5}$ content in HfO_2, the dielectric constant increases with higher $YO_{1.5}$ content. Once the cubic phase is fully stabilized, further addition of the lower-k $YO_{1.5}$ decreases the effective permittivity of HfO_2 again.

However, when directly comparing PMA against PDA samples, PDA samples exhibit lower P_r values and the P_r evolution slightly shifts to higher $YO_{1.5}$ content. A similar shift is observed when comparing the dielectric constant at corresponding $YO_{1.5}$ content. The mechanical confinement offered by the top electrode during the crystallization of the PMA samples can serve as an explanation. As can be seen from the weighing of the integral intensity of monoclinic against higher symmetry reflections in Fig. 6(c) and the direct comparison of GI-XRD diffractograms in Fig. 7, the monoclinic phase in HfO_2 can effectively be suppressed utilizing PMA processing. This suppression mechanism of monoclinic HfO_2 in thin films by a mechanically confined crystallization (e.g. reported for TiN/HfO_2 gate stacks[28]) was identified to be the origin of the orthorhombic, ferroelectric, phase in SiO_2-doped HfO_2.[5] The increased P_r observed in PMA samples at low $YO_{1.5}$ content suggests a larger ferroelectric phase fraction due to the suppressed monoclinic phase. However, even though PDA samples exhibit lower P_r, they still show the presence of ferroelectricity, suggesting that the presence of a top electrode ("cap") is preferred, but not mandatory, for the formation of the ferroelectric phase in Y:HfO_2 thin films. This advantageous discrepancy to ferroelectricity in Si:HfO_2,[5] for which PMA treatment was found to be necessary, may be explained by the difference in crystallization temperatures of both systems. The crystallization

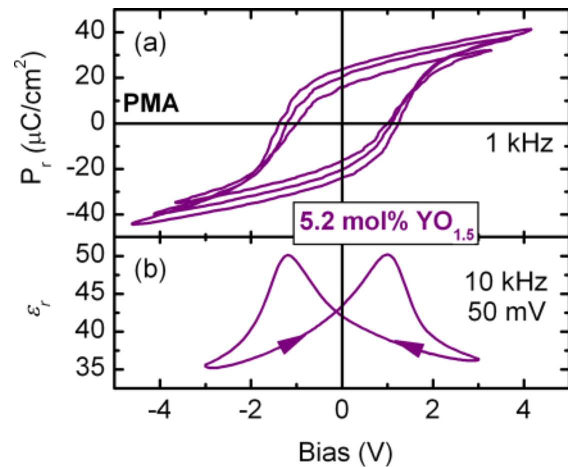

FIG. 4. (Color online) A characteristic transformation from sub-loop behavior to saturation with increasing P-V sweep voltage (a), as well as ferroelectric capacitance peaks in dual sweep C-V (b) are observed for TiN/10 nm 5.2 mol% Y:HfO_2/TiN MIM capacitors.

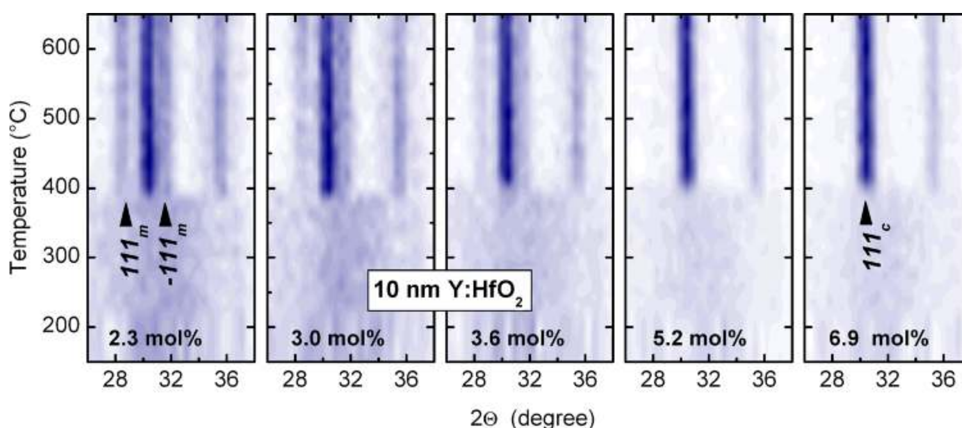

FIG. 3. (Color online) HT-XRD analysis of 10 nm HfO_2 thin films with $YO_{1.5}$ admixture ranging from 2.3 to 6.9 mol%. With increasing $YO_{1.5}$ content the monoclinic phase in HfO_2 is suppressed, whereas crystallization temperature remains at approximately 400 °C.

Downloaded 06 Nov 2012 to 131.188.201.33. Redistribution subject to AIP license or copyright; see http://jap.aip.org/about/rights_and_permissions

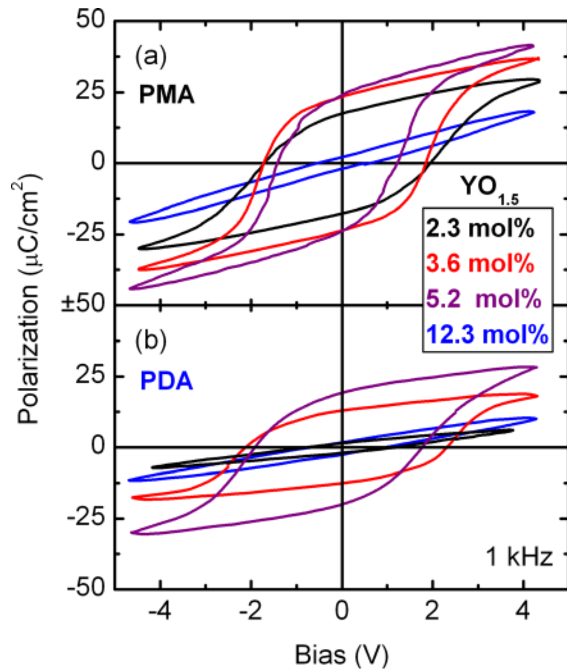

FIG. 5. (Color online) P-V hysteresis loops acquired on 10 nm Y:HfO_2 MIM capacitors treated with PMA (a) and PDA (b) processing clearly exhibit ferroelectric nature. For PDA treated samples a linear dielectric response is observed at low $YO_{1.5}$ content. For high $YO_{1.5}$ admixture to HfO_2 a linear dielectric response is observed for both processing schemes.

of Si:HfO_2 requires temperatures in excess of 700 °C and may therefore lead to a more rapid formation of stable crystalline phases instead of quenchable, metastable intermediates.

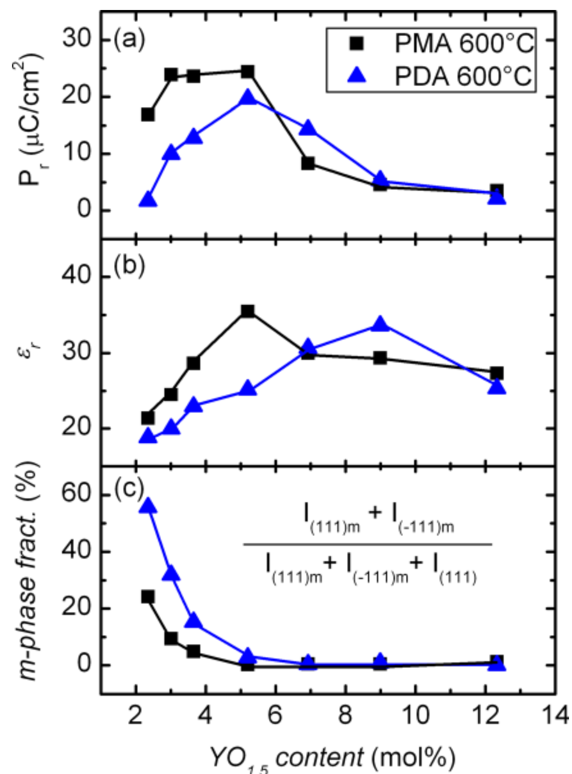

FIG. 6. (Color online) Remanent polarization (a) and dielectric permittivity (b) maxima for PMA and PDA treated Y:HfO_2 MIM capacitors are contrasted to the monoclinic phase fraction (c) evaluated from weighing the integral intensity of monoclinic against higher symmetry reflections.

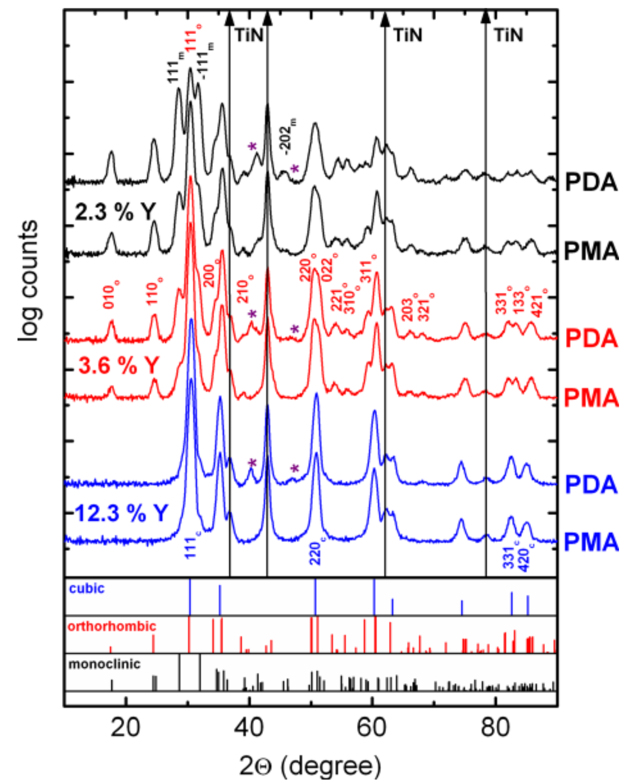

FIG. 7. (Color online) GI-XRD diffractograms of Y:HfO_2 samples reveal the coexistence of monoclinic and orthorhombic phase for low $YO_{1.5}$ doping and complete stabilization of the cubic phase for higher doping content. When directly comparing PMA against PDA treated samples a higher monoclinic phase fraction for PDA samples is observed. Reference pattern are computed from ab initio calculations presented by Lowther *et al.*[31] on HfO_2 phase stability (cubic Fm3m, orthorhombic Pbc2_1, monoclinic P2_1/c). D-spacing was adjusted. For better visibility, reference patterns were scaled to the 2nd highest square root intensity (highest intensity for all patterns: 111 reflections). Stars indicate Pt reflections.

Stabilization of the cubic phase in the predominantly monoclinic HfO_2 by $YO_{1.5}$ admixture is widely accepted in literature and has been reported several times.[9–17] However, considering the occurrence of ferroelectricity in Y:HfO_2 thin films, a simple monoclinic/cubic phase mixture or intermediate tetragonal phases seem contradictory, since neither the cubic/tetragonal nor the monoclinic phases in HfO_2 possess ferroelectric space groups.[29] A close examination of the GI-XRD diffractograms presented in Fig. 7 revealed the presence of an orthorhombic phase, whose phase fraction increases against the monoclinic phase until a full stabilization of the cubic phase is reached for high $YO_{1.5}$ content. These findings are in good agreement with data on Y:HfO_2 thin films shown by Rauwel *et al.*[21] and Dubourdieu *et al.*,[22] who observed a possibly orthorhombic phase coexisting with the monoclinic phase until a stable cubic phase is reached. This orthorhombic phase, however, was identified as centrosymmetric Pbca and was seemingly not tested for ferroelectric properties.

On the basis of the electrical data presented, it seems likely that this orthorhombic phase can be assigned to the non-centrosymmetric, and therefore potentially ferroelectric, space group Pbc2_1. This phase has already been observed in the closely related PSZ[30] and was predicted for HfO_2[31] by an

Downloaded 06 Nov 2012 to 131.188.201.33. Redistribution subject to AIP license or copyright; see http://jap.aip.org/about/rights_and_permissions

ab initio approach. It can be separated from the monoclinic and cubic phase by the characteristic features labeled in Fig. 7. This analogy to ferroelectric Si:HfO_2 supports the hypothesis that the structural origin of spontaneous polarization in doped HfO_2 is linked to the stabilization of this particular phase and does not originate from the dopant itself.[5]

The anti-ferroelectric like behavior observed for the fully stabilized Si:HfO_2, however, was not observed in the Y:HfO_2 system within our experimental conditions. Tomida *et al.*[16] clearly distinguished the tetragonal Si:HfO_2 from the cubic Y:HfO_2 system. This further supports the hypothesis that the field driven phase transition observed in Si:HfO_2[5] is related to the tetragonal phase stabilized for high SiO_2 doping and is not present in the cubic configuration favored by $YO_{1.5}$ incorporation.

In the context of ferroelectricity being present in Y:HfO_2, it is interesting to note that unusual threshold voltage shifts have been observed for Y:HfO_2 based transistors under constant voltage stress.[23] The phenomenon described in the present work could serve as an explanation, since even residual ferroelectricity being present in the gate stack would counteract the usual polarity correlation of threshold voltage shift and stress voltage by slow polarization reversal.

CONCLUSION

In conclusion, we have demonstrated the stabilization of a ferroelectric phase in 10 nm thick, atomic layer deposited Y:HfO_2 thin films for doping levels below 8 mol% $YO_{1.5}$. The origin of ferroelectricity was attributed to an orthorhombic phase of space group $Pbc2_1$, which was found to coexist with the monoclinic phase until complete stabilization of the cubic phase is reached. Given the vast industry experience integrating HfO_2-based thin films, ferroelectricity in Y:HfO_2 has the potential to enable high density ferroelectric memories. Besides its thermal stability on contact with Si, Y:HfO_2 offers excellent scaling potential due to its large bandgap and highly conformal deposition processes (3D integration capability), rendering it superior to commonly integrated ferroelectrics in microelectronic devices.

ACKNOWLEDGMENTS

Prof. S. Teichert is acknowledged for RBS measurements and M. Mildner is acknowledged for TEM micrographs. We would like to thank Prof. K. Dörr and Prof. A. Kersch for helpful discussions. The work for this paper was supported within the scope of technology development by the EFRE fund of the European Community and by funding from the Free State of Saxony (Project MERLIN). The authors are responsible for the content of the paper.

[1]K. Kim and S. Lee, J. Appl. Phys. **100**, 51604 (2006).
[2]X. Zhao and D. Vanderbilt, Phys. Rev. B **65**, 233106 (2002).
[3]K. Kita, K. Kyuno, and A. Toriumi, Appl. Phys. Lett. **86**, 102906 (2005).
[4]T. S. Böscke, S. Govindarajan, P. D. Kirsch, P. Y. Hung, C. Krug, B. H. Lee, J. Heitmann, U. Schröder, G. Pant, B. E. Gnade, and W. H. Krautschneider, Appl. Phys. Lett. **91**, 72902 (2007).
[5]T. S. Böscke, J. Müller, D. Bräuhaus, U. Schröder, and U. Böttger, Appl. Phys. Lett. **99**, 102903 (2011).
[6]J. Müller, T. S. Böscke, D. Bräuhaus, U. Schröder, U. Böttger, J. Sundqvist, P. Kücher, T. Mikolajick, and L. Frey, Appl. Phys. Lett. **99**, 112901 (2011).
[7]C.-K. Lee, E. Cho, H.-S. Lee, C. S. Hwang, and S. Han, Phys. Rev. B **78**, 12102 (2008); G. H. Chen, Z. F. Hou, X. G. Gong, and Quan Li, J. Appl. Phys. **104**, 74101 (2008).
[8]R. C. Garvie, R. H. J. Hannink, and R. T. Pascoe, Nature **258**, 703 (1975).
[9]S. V. Ushakov, C. E. Brown, and A. Navrotsky, J. Mater. Res. **19**, 693 (2004).
[10]J. Y. Dai, P. F. Lee, K. H. Wong, H. L. W. Chan, and C. L. Choy, J. Appl. Phys. **94**, 912 (2003).
[11]M. Komatsu, R. Yasuhara, H. Takahashi, S. Toyoda, H. Kumigashira, M. Oshima, D. Kukuruznyak, and T. Chikyow, Appl. Phys. Lett. **89**, 172107 (2006).
[12]J. Niinisto, K. Kukli, T. Sajavaara, M. Ritala, M. Leskela, L. Oberbeck, J. Sundqvist, and U. Schröder, Electrochem. Solid-State Lett. **12**, G1–G4 (2009).
[13]Q. Tao, G. Jursich, P. Majumder, M. Singh, W. Walkosz, P. Gu, R. Klie, and C. Takoudis, Electrochem. Solid-State Lett. **12**, G50–G53 (2009).
[14]L. Shi, Y. Zhou, J. Yin, and Z. Liu, J. Appl. Phys. **107**, 14104 (2010).
[15]Z. K. Yang, W. C. Lee, Y. J. Lee, P. Chang, M. L. Huang, M. Hong, K. L. Yu, M.-T. Tang, B.-H. Lin, C.-H. Hsu, and J. Kwo, Appl. Phys. Lett. **91**, 202909 (2007).
[16]K. Tomida, K. Kita, and A. Toriumi, Appl. Phys. Lett. **89**, 142902 (2006).
[17]T. Rössler, J. Gluch, M. Albert, and J. W. Bartha, Thin Solid Films **518**, 4680 (2010).
[18]D.W. Stacy and D. R. Wilder, J. Am. Ceram. Soc. **58**, 285 (1975); M. F. Trubelja and V. S. Stubican, J. Am. Ceram. Soc. **71**, 662 (1988).
[19]M. Yashima, H. Takahashi, K. Ohtake, T. Hirose, M. Kakihana, H. Arashi, Y. Ikuma, Y. Suzuki, and M. Yoshimura, J. Phys. Chem. Solids **57**, 289 (1996).
[20]H. Fujimori, M. Yashima, S. Sasaki, M. Kakihana, T. Mori, M. Tanaka, and M. Yoshimura, Chem. Phys. Lett. **346**, 217 (2001).
[21]E. Rauwel, C. Dubourdieu, B. Hollander, N. Rochat, F. Ducroquet, M. D. Rossell, G. Van Tendeloo, and B. Pelissier, Appl. Phys. Lett. **89**, 12902 (2006).
[22]C. Dubourdieu, E. Rauwel, H. Roussel, F. Ducroquet, B. Hollander, M. Rossell, G. Van Tendeloo, S. Lhostis, and S. Rushworth, J. Vac. Sci. Technol. A **27**, 503 (2009).
[23]S. Motoyuki, K. Satoshi, and M. Takeo, Jap. J. Appl. Phys. **49**, 04DC24 (2010).
[24]K. J. Hubbard and D. G. Schlom, J. Mater. Res. **11**, 2757 (1996).
[25]J. Müller, T. S. Böscke, U. Schröder, M. Reinicke, L. Oberbeck, D. Zhou, W. Weinreich, P. Kücher, M. Lemberger, and L. Frey, Microelectronic Engineering **86**, 1818 (2009).
[26]S. L. Miller, R. D. Nasby, J. R. Schwank, M. S. Rodgers, and P. V. Dressendorfer, J. Appl. Phys. **68**, 6463 (1990).
[27]D. Bolten, O. Lohse, M. Grossmann, and R. Waser, Ferroelectrics **221**, 251 (1999).
[28]D. H. Triyoso, P. J. Tobin, B. E. White, J. R. R. Gregory, and X. D. Wang, Appl. Phys. Lett. **89**, 132903 (2006).
[29]D. B. Litvin, Acta Crystallogr. **A42**, 44 (1986).
[30]E. H. Kisi, C. J. Howard, and R. J. Hill, J. Am. Ceram. Soc. **72**, 1757 (1989).
[31]J. E. Lowther, J. K. Dewhurst, J. M. Leger, and J. Haines, Phys. Rev. B **60**, 14485 (1999).

Downloaded 06 Nov 2012 to 131.188.201.33. Redistribution subject to AIP license or copyright; see http://jap.aip.org/about/rights_and_permissions